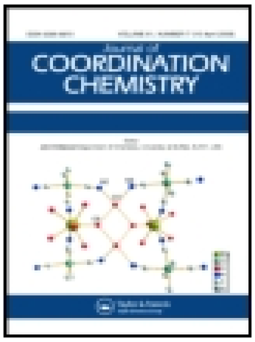

Journal of Coordination Chemistry

ISSN: 0095-8972 (Print) 1029-0389 (Online) Journal homepage: http://www.tandfonline.com/loi/gcoo20

Syntheses and characterization of the vanadium trimer $(V_3(\mu_3\text{-}O)O_2)(\mu_2\text{-}O_2P(CH_2C_6H_5)_2)_6(4,4'\text{-bipyridine})$ and the vanadium hexamer $[(V_3(\mu_3\text{-}O)O_2)(\mu_2\text{-}O_2P(CH_2C_6H_5)_2)_6]_2(\mu_2\text{-}N^1,N^2\text{-di(pyridin-4-yl)oxalamide})$

John S. Maass, Zhichao Chen, Matthias Zeller & Rudy L. Luck

To cite this article: John S. Maass, Zhichao Chen, Matthias Zeller & Rudy L. Luck (2016): Syntheses and characterization of the vanadium trimer $(V_3(\mu_3\text{-}O)O_2)(\mu_2\text{-}O_2P(CH_2C_6H_5)_2)_6(4,4'\text{-bipyridine})$ and the vanadium hexamer $[(V_3(\mu_3\text{-}O)O_2)(\mu_2\text{-}O_2P(CH_2C_6H_5)_2)_6]_2(\mu_2\text{-}N^1,N^2\text{-di(pyridin-4-yl)oxalamide})$, Journal of Coordination Chemistry, DOI: 10.1080/00958972.2016.1188383

To link to this article: http://dx.doi.org/10.1080/00958972.2016.1188383

Publisher: Taylor & Francis

Journal: *Journal of Coordination Chemistry*

DOI: http://dx.doi.org/10.1080/00958972.2016.1188383

Syntheses and characterization of the vanadium trimer $(V_3(\mu_3\text{-}O)O_2)(\mu_2\text{-}O_2P(CH_2C_6H_5)_2)_6$(4,4'-bipyridine) and the vanadium hexamer $[(V_3(\mu_3\text{-}O)O_2)(\mu_2\text{-}O_2P(CH_2C_6H_5)_2)_6]_2(\mu_2\text{-}N^1,N^2)$-di(pyridin-4-yl)oxalamide)

JOHN S. MAASS†, ZHICHAO CHEN†, MATTHIAS ZELLER‡§ and RUDY L. LUCK*†

†Department of Chemistry, Michigan Technological University, 1400 Townsend Drive, Houghton, MI 49931, USA
‡Department of Chemistry, Youngstown State University, 1 University Plaza, Youngstown, Ohio 44555, USA
§Purdue University, Department of Chemistry, 560 Oval Drive, West Lafayette, IN 47907-2084, USA

Reacting $VO(acac)_2$ with six equivalents of dibenzylphosphinic acid in the presence of 4,4'-bipyridine or μ_2-N^1,N^2-di(pyridin-4-yl)oxalamide leads to trimeric $(V_3(\mu_3\text{-}O)O_2)(\mu_2\text{-}O_2P(CH_2C_6H_5)_2)_6$(4,4'-bipyridine) or the hexamer $[(V_3(\mu_3\text{-}O)O_2)(\mu_2\text{-}O_2P(CH_2C_6H_5)_2)_6]_2(\mu_2$-$N^1$,$N^2$-di(pyridin-4-yl)oxalamide). The complexes were characterized by spectroscopic (FTIR and ^{1}H NMR spectroscopies), TGA and by single crystal X-ray diffraction measurements. The structures consist of a planar central core where three vanadium ions are arranged in the form of a quasi-isosceles triangle and contain an interstitial O which is multiply bonded to one V and weakly interacting at different bond distances to the remaining two V ions.

Keywords: Vanadium hexamers; Vanadium trimers; Phosphinate ligands; 4,4'-Bipyridine; *N*,*N*'-Disubstituted oxalamide; N^1,N^2-Di(pyridin-4-yl)oxalamide; Bridging ligands

---

*Corresponding author. Email: rluck@mtu.edu

1. Introduction

While VO(acac)$_2$ has been reported to form weakly coordinating monomeric adducts with ligands *trans* to the $[V^{IV}O]^{2+}$ moiety [1], there has only been one published report of dimers featuring a linkage with 4,4'-bipyridine. This was with a substituted derivative [VO(OEt)L] (H_2L = (Z)-2-hydroxy-*N*-((E)-2-hydroxybenzylidene)benzohydrazonic acid), resulting in $[VO(OEt)L]_2(\mu\text{-}4,4'\text{-bipy})$ identified crystallographically with an *R* value of 11% [2]. Two additional dimers with bridging ligands containing ethylene and ethyl groups between the pyridyl ligands were also reported in this paper. The crystal structure of the ethylene derivative was affected by disorder and best refined to an *R* value of 18% [2]. Lower valent dimers of vanadium, *i.e.*, V^{III} in $[(Cp_2V)_2(\mu_2\text{-}py_2N_2)]$, $[(Cp^*{}_2V)_2(\mu_2\text{-}4\text{-bipy})][BPh_4]_2$ and $[(Cp^*{}_2V)_2(\mu_2\text{-}py_2C_2)][BPh_4]_2$ have also been characterized and here the spacers between the pyridyl groups were N_2 and C_2 [3].

The syntheses of two V^{IV} trimers $(V_3(\mu_3\text{-O})O_2)(\mu_2\text{-}O_2P(CH_2C_6H_5)_2)_6(H_2O)$, **1**, and $(V_3(\mu_3\text{-O})O_2)(\mu_2\text{-}O_2P(CH_2C_6H_5)_2)_6(py)$, **2**, [4] and the tetramer $V_4(\mu_3\text{-O})_4(\mu_2\text{-}O_2P(Bn)_2)_4(O_4)$ [5] all containing the $[VO]^{2+}$ moiety were also previously detailed. The trimers are of a non-classical nature based on the C_{2v} symmetry for the three vanadium ions and the triply bridging oxide ligand [4]. The trimers exhibit a very weak magnetic interaction between the vanadyl centers based on magnetization measurements at 2 and 4 K [4]. Similar to VO(acac)$_2$, the trimers contain an easily displaced ligand and thus the synthesis of dimers of the trimers might be possible with a suitable bridging ligand. Herein is reported that 4,4'-bipyridine could not bridge between two V trimers but that N^1,N^2-di(pyridin-4-yl)oxalamide was sufficiently long to overcome steric conflicts and afford the desired hexamer. This ligand has been the subject of several recent crystallographic studies including its structure determination [6], as a deprotonated cation salt of perchlorate [7] and an octamolybdate anion [8], and as a bridging ligand resulting in rectangular tetrameric arrays of Ru$_4$ [9, 10] and Rh$_4$ [11, 12]. Additionally, various clusters have been synthesized featuring *N*,*N*'-disubstituted oxalamides [13, 14]. The complexes reported herein are characterized by elemental analysis, single-crystal X-ray crystallography and TGA measurements.

2. Experimental

2.1. *Materials*

Chemicals were purchased from Sigma-Aldrich Chemicals and solvents were purified as needed. Dichloromethane was dried by distillation over CaH_2 under nitrogen. Elemental analyses were conducted by Galbraith Laboratories, Knoxville, TN. IR and NMR spectra were recorded on a Perkin Elmer Spectrum One spectrometer (neat) and a Varian 400 MHz NMR instrument, respectively. The TGA analyses were conducted on Shimadzu TGA-50 and DSC-50 analyzers. Dibenzylphosphinic acid [15] and VO(acac)$_2$ (VO(acac)$_2$ confirmed by FTIR spectroscopy [4]) were prepared according to the cited literature [16, 17]. The synthesis and characterization of N^1,N^2-di(pyridin-4-yl)oxalamide has been reported previously [6] and an alternative route, which differed in the use of oxalic acid dihydrate instead of the oxalic acid diethyl ester, is outlined below.

2.2. *Synthesis of* $(V_3(\mu_3\text{-}O)O_2)(\mu_2\text{-}O_2P(CH_2C_6H_5)_2)_6((C_5H_4N)_2)$ *(3)*

4,4'-Bipyridine (0.010 g, 0.064 mmol), VO(acac)$_2$ (0.051 g, 0.192 mmol) and bis(benzyl)phosphinic acid (0.095 g, 0.384 mmol) were dissolved in 10 mL of dry CH_2Cl_2 under an atmosphere of nitrogen. The green solution was stirred at room temperature for two hours after which the solution had become light blue. This solution was then filtered and hexanes were added to the filtrate to obtain a blue precipitate which was filtered and dried under vacuum to give 0.077 grams (0.042 mmol, 65.6% based on VO(acac)$_2$) of $(V_3(\mu_3\text{-}O)O_2)(\mu_2\text{-}O_2P(CH_2C_6H_5)_2)_6$(4,4'-bipyridine) (**3**). Anal. Calcd for $C_{94}H_{92}N_2O_{15}P_6V_3\cdot 0.5(CH_2Cl_2)$: C, 60.67; H, 5.01. Found: C, 60.85; H, 4.94. IR (Supporting Information figure S1, neat, cm^{-1}) 3058 (vw), 3028 (w), 2907 (vw), 1603 (m), 1533 (w), 1496 (m), 1454 (m), 1403 (m), 1234 (m), 1189 (s), 1162 (s), 1103 (m), 1067 (m), 1024 (vs), 994 (s), 926 (s), 842 (vs), 804 (vs), 732 (m), 696 (vs). ^{1}NMR (figure S3, CD_2Cl_2) 1.79 (br, CH_2), 7.20 (br, arene-*H*); (figure S4, $CDCl_3$) 1.94 (br, CH_2), 7.17 (br, arene-*H*).

2.3. *Synthesis of* N^1,N^2-di(pyridin-4-yl)oxalamide *(4)*

Oxalic acid dihydrate (5.01 g, 39.74 mmol), 10 mL of ethanol and 30 mL of benzene were heated at reflux overnight in a flask fitted with a Dean-Stark condenser; 4-aminopyridine (7.48 g, 79.47 mmol) was added to this mixture which was heated at reflux for six hours. The white precipitate that formed was filtered off and rinsed with a small amount of benzene. It was then dried under vacuum resulting in 2.45 grams (10.11 mmol, 25.4% yield based on oxalic acid dihydrate) of N^1,N^2-di(pyridin-4-yl)oxalamide (**4**).

2.4. ***Synthesis of*** $((V_3(\mu_3\text{-}O)O_2)(\mu_2\text{-}O_2P(CH_2C_6H_5)_2)_6)_2(C_{12}H_{10}N_4O_2)$ ***(5)***

N^1,N^2-di(pyridin-4-yl)oxalamide (0.010 g, 0.046 mmol), bis(benzyl)phosphinic acid (0.136 g, 0.550 mmol) and VO(acac)$_2$ (0.073 g, 0.275 mmol) were dissolved in 15 mL of dry CH_2Cl_2 under an atmosphere of nitrogen and stirred overnight. The blue solution was then filtered and hexanes were added to the filtrate causing a blue precipitate to form which was subsequently filtered off. The precipitate was dried under vacuum resulting in 0.08 grams (0.022 mmol, 48.8% yield based on VO(acac)$_2$) of $((V_3(\mu_3\text{-}O)O_2)(\mu_2\text{-}O_2P(CH_2C_6H_5)_2)_6)_2(C_{12}H_{10}N_4O_2)$ (**5**). Anal. Calcd for $C_{180}H_{178}N_4O_{32}P_{12}V_6\cdot 1.5(CH_2Cl_2)$: C, 58.69; H, 4.91. Found: C, 58.61; H, 4.92. IR (Supporting Information figure S2, neat, cm^{-1}) 3351 (vw), 3067 (vw), 3030 (w), 2905 (vw), 1705 (m), 1602 (sh), 1583 (m), 1533 (w), 1496 (m), 1453 (m), 1403 (m), 1328 (br), 1234 (m), 1187 (s), 1163 (s), 1104 (m), 1067 (m), 1026 (vs), 996 (s), 922 (s), 841 (vs), 805 (vs), 733 (m), 696 (vs). ^{1}NMR (figure S5, $CDCl_3$) 2.34 (br, CH_2), 7.17 (br, arene-*H*).

2.5. ***X-ray crystallography***

X-ray quality crystals for both compounds were grown by slow diffusion of pentane into methylene chloride solutions of **3** and **5** in H-tubes. Diffraction data for all compounds were collected using a Bruker AXS SMART APEX CCD diffractometer using monochromatic Mo Kα radiation with the omega scan technique. Single crystals of **3** and **5** were mounted on Mitegen micromesh supports using mineral oil flash-cooled to 100 K. Data were collected, unit cells determined, and the data integrated and corrected for absorption and other systematic errors using the Apex2 suite of programs [18]. The structures were solved by direct methods and refined by full matrix least squares against F^2 with all reflections using SHELXL [19]. For **5**, reverse Fourier transform methods as implemented in the program Squeeze [20] were utilized to correct for the contribution of disordered solvent molecules to the scattering factors. Final figures of merit for the two structures are listed in table 1.

3. Results and discussion

3.1. *Synthesis of 3 and 5*

Compounds **3** and **5** were synthesized using a method that was previously employed for the syntheses of the H_2O and py adducts of $(V_3(\mu_3\text{-}O)O_2)(\mu_2\text{-}O_2P(CH_2C_6H_5)_2)_6$ [4], scheme 1. When $VO(acac)_2$ is dissolved in methylene chloride with six equivalents of bis(benzyl)phosphinic acid and one equivalent of 4,4'-bipyridine, the nonclassical vanadium(IV) cluster, $(V_3(\mu_3\text{-}O)O_2)(\mu_2\text{-}O_2P(CH_2C_6H_5)_2)_6((C_5H_4N)_2)$, **3**, readily forms. This reaction was attempted to verify if 4,4'-bipyridine was capable of bridging two of these trimers but **3** with only one end of the bipyridine group coordinated analogous to the aforementioned H_2O and py derivatives [4] was obtained. Substitution reactions involving reacting 4,4'-bipyridine with either trimers **1** or **2** in the appropriate stoichiometries were not successful in producing either a dimer or the monosubstituted derivative. It appears that 4,4'-bipyridine is too short to bridge the trimers and there may be too much steric repulsion between benzyl groups on opposing trimers resulting in the mono-substituted derivative **3**. It was then decided to utilize N^1,N^2-di(pyridin-4-yl)oxalamide which was longer and should reduce the amount of steric interactions between the two clusters. This approach, which resulted in **5**, was successful and the desired dimer of trimers was thus obtained, scheme 1.

The three $[VO^{2+}]$ moieties in the trimer absorb at slightly different positions in their FTIR spectra [4] as one of these has a stronger *trans*-donating ligand. Two bands at 1024 and 995 cm^{-1} for $V_3(\mu_3\text{-}O)O_2)(\mu_2\text{-}O_2P(CH_2C_6H_5)_2)_6(H_2O)$ and 1026 and 989 cm^{-1} for $V_3(\mu_3\text{-}O)O_2)(\mu_2\text{-}O_2P(CH_2C_6H_5)_2)_6(C_5H_4N)$ were noted with the lower resonances ascribed to the $[VO^{2+}]$ moiety *trans* to H_2O and py, respectively [4]. For **3** and **5**, the relevant absorptions occur at 1024 and 994 cm^{-1} and 1026 and 996 cm^{-1}, respectively, indicating that the *trans* ligand in these complexes is not as strong a σ-donor as the py ligand. As there would not appear to be significant electronic reasons for reduced basicity, steric hindrance may be responsible. A weak absorption at 3351 cm^{-1} in the FTIR spectrum of **5** can be assigned to the N-H bond stretch. There is also evidence of the C=O bond vibration at 1705 cm^{-1}.

Attempts were made to obtain the ^1H NMR spectra for these paramagnetic compounds. There was evidence for the attached ligand with **3** if dissolved in CD_2Cl_2 (figure S3) and in $CDCl_3$ (figure S4) in the form of broad resonances at $\delta = 1.79$ and 1.94, respectively, for hydrogens attached to the CH_2 groups. The phenyl hydrogens in **3** appeared as broad signals at δ

= 7.20 and 7.17 in CD_2Cl_2 and in $CDCl_3$, respectively. Hydrogens on the bipy ligand of **3** were not observed. Complex **5** in $CDCl_3$, figure S5, contained broad signals at $\delta = 2.34$ and 7.17 for the CH_2 and phenyl hydrogens, respectively, but there were possible signs of decomposition by a small bump at $\delta = 2.90$ which may indicate ligand dissociation. Peaks for the bridging group, *i.e.*, N^1,N^2-di(pyridin-4-yl)oxalamide, were not observed. Both **3** and **5** decomposed in DMSO judging by the appearance of sharp signals in their NMR spectra indicative of dissociated phosphinate ligands and bipy for **3** (figure S6) and dissociated phosphinate ligands and N^1,N^2-di(pyridin-4-yl)oxalamide for **5** (figure S7).

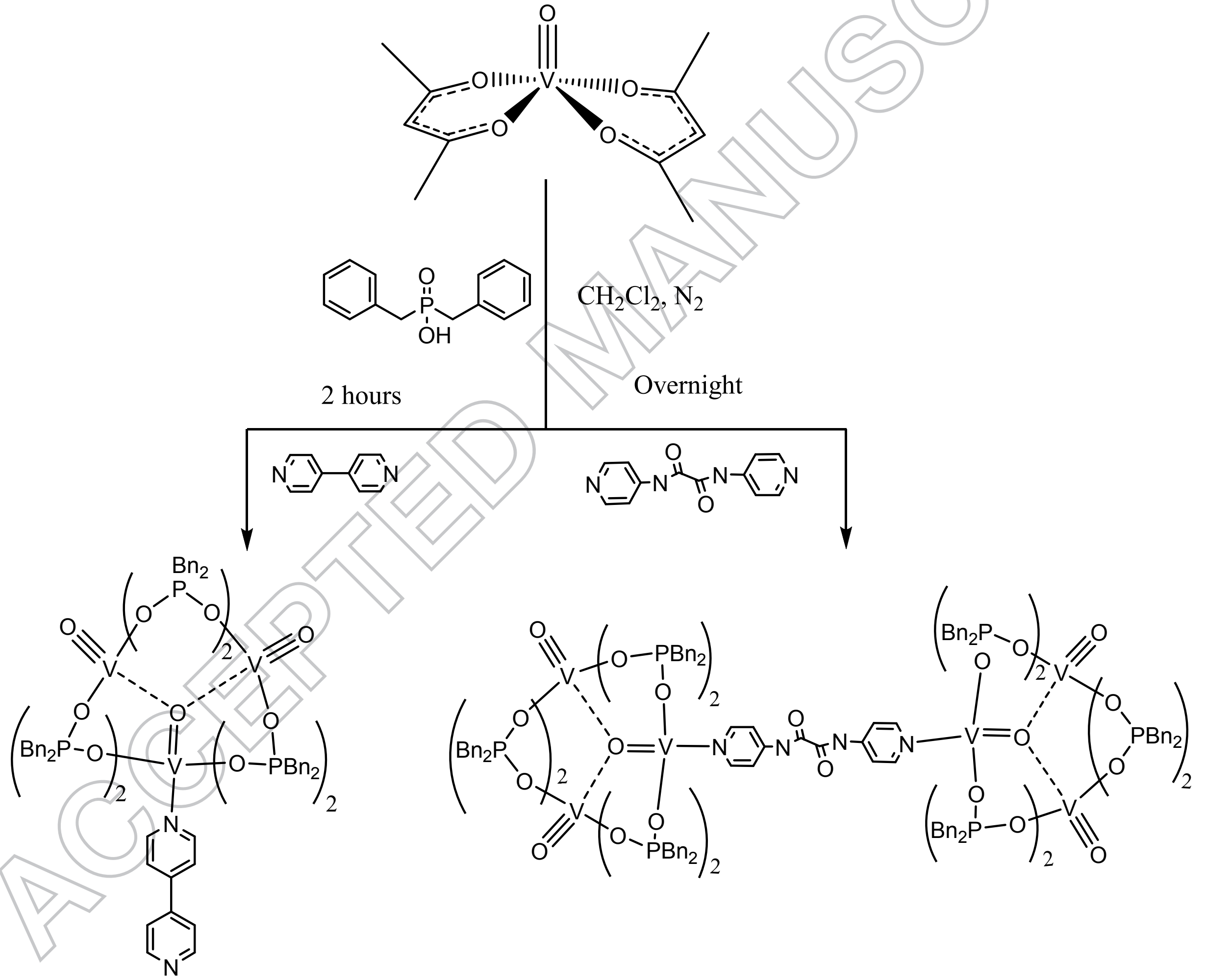

3

5

Scheme 1. Preparation of **3** and **5**.

3.2. *Crystallography*

Mercury [21] thermal ellipsoid representations of **3** and **5** are given in figures 1 and 2, respectively. Compound **3** crystallized as a solvate with two molecules of dichloromethane, *i.e.*, **3**·$2CH_2Cl_2$, which were disordered. With one CH_2Cl_2, the Cl atoms were fixed and the CH_2 fragment was disordered over two positions. The other dichloromethane was refined with 50% occupancies and it was located at two sites in the unit cell both being near inversion points. One of the benzene rings in **3** was also disordered and this was accounted for by setting the occupancy of the atoms in each ring to the same value and then refining the occupancy of those atoms in the two rings to sum up to one. Compound **5** also contained solvent molecules which proved difficult to refine. Reflections for these were corrected using the squeeze routine leaving behind a void volume of 2760 Å^3 out of a total cell volume of 10,627 Å^3 (or 26%). This may correspond to roughly 20 CH_2Cl_2 molecules per unit cell and a density of 1.387 g/cm^3 which is similar to that obtained for **3** at 1.401 g/cm^3.

Both **3** and **5** consist of quasi-isosceles triangular arrangements of the three [VO^{2+}] moieties such that one of these points inwards while the other two are oriented outside of the vanadium triangle as illustrated in figures 1 and 2, respectively. Bond valence sum calculations [22] establish the +4 oxidation state for all V ions in the two compounds, table S1 for **3** and table S2 for **5**. In each complex adjacent vanadium ions are bridged by two dibenzylphosphinate ligands. One molecule of $(V_3(\mu_3\text{-}O)O_2)(\mu_2\text{-}O_2P(CH_2C_6H_5)_2)_6((C_5H_4N)_2)$, **3**, together with two CH_2Cl_2 comprise the asymmetric unit whereas **5** is arranged around an inversion point located at the C-C linkage in the oxalamide moiety. The bipy in **3** twists slightly, possibly to accommodate a close interaction at 2.280(5) Å between a hydrogen (*i.e.*, H89, figure 1) attached to C that is adjacent to the bonded N and O13 in the phosphinate ligand. The two py rings in the bipy ligand are not coplanar and are at an interplanar angle of 42.41(5)°. In **5**, the planes for the two py groups in the bridging ligand are parallel and separated by a distance of **0.975(5) Å** *[au: please check]*. The atoms constituting the oxalamide group and both N and C in the two py groups are co-planar (crystallographically imposed). The planes of both py groups are twisted by 20.58(5)° from this oxalamide plane. The hydrogens situated on the *ortho* C in the bridging ligand in **5** are at 2.311(5) and 2.333(5) Å from the nearest O on the bridging phosphinate ligands, resulting in a more symmetrical bonding interaction for the bridging ligand as opposed to that for the bipy ligand in **3**.

It is interesting to compare equivalent distances and angles for previously published vanadium trimers **1** and **2** to those obtained for **3** and **5** and some pertaining to the central cores are listed in table 4. There are no significant differences in the equivalent V to O (terminal) or V to O (interstitial) distances with **2**, **3** and **5**, though it appears the equivalent data for **1** are significantly shorter. Of note is the fact that the bond distance for the V_1=O_1 moiety *trans* to L is significantly longer in all cases. There are also significant differences in the bond distances labelled as V_1-L ranging from the shortest with L = H_2O in **1** at 2.307(4) Å to the longest with L = bipy in **3** at 2.409(2) Å. The short distance for the V_1 to N in **2** at 2.350(3) Å compared to that at 2.409(2) and 2.385(2) Å for **3** and **5**, respectively, may be related to the fact that the smaller py ligand in **2** can twist to avoid steric interactions and thus can bond more closely than the larger ligands in **3** and **5** as evident in the angles between the planes of the "py" groups and that from three V ions and O_1 at 47.41(5), 22.81(5) and 26.42(5)° for **2**, **3** and **5**, respectively.

Lone pairs from the interstitial O_1 for **3** and **5** interact weakly with the other two V ions at different distances and those of **1** (2.57(2) and 2.74(2) Å) and **3** (2.570(1) and 2.728(1) Å) not being significantly different between each other but different from those in **2** (2.510(2) and 2.830(3) Å) and **5** (2.526(2) and 2.817(2) Å), which were similar. This interstitial O to V atom interaction is responsible for the significantly longer V to V distance between V_2 and V_3 noted in table 4. Equivalent angles within the central core are similar and the three interstitial angles add to 360° establishing a planar core. The three angles described by the V ions together with the three distances (both containing two similar values and one significantly different) in table 4 establishes a quasi-isosceles geometry for all these complexes.

3.3. *Thermal analysis*

The thermal decompositions of $V_3(\mu_3\text{-O})O_2)(\mu_2\text{-}O_2P(CH_2C_6H_5)_2)_6$(4,4'-bipyridine), **3**, and $(V_3(\mu_3\text{-O})O_2)(\mu_2\text{-}O_2P(CH_2C_6H_5)_2)_6)_2$($N^1$,$N^2$-dipyrid-4-yl oxalamide), **5**, were studied by TGA after drying by being kept at room temperature under vacuum overnight. The experiments were conducted under oxygen at a heating rate of 10 °C/min. The samples were heated to 600 °C and kept for 30 min to complete the decomposition. For **3**, figure 3, a weight loss corresponding to 4,4'-bpy ligand (calc. 8.5%, obs. 8.1%) was observed from 160-250 °C. Weight loss of 8.6% from 250-350 °C could be the dissociated dibenzylphosphinic acid as verified independently for the related **1** and **2** [4]. After that, the compound decomposed further and gave a final weight of 38.6% corresponding to $VO(PO_3)_2$ (calc. 36.9%).

Compound **5**, figure 4, revealed a small decrease in weight (1.9%) before 200 °C presumably corresponding to moisture or solvents. A weight loss of 8.1% was observed from 200-260 °C possibly due to dissociation of the bridging N^1,N^2-dipyrid-4-yl oxalamide (calc. 6.8%), followed by dissociation of dibenzylphosphinic acid from 260-350 °C. The compound is stable at 600 °C with a final weight of 37.1% corresponding to $VO(PO_3)_2$ (calc. 37.6%).

4. Conclusion

Attempts to connect the vanadium trimer "$V_3(\mu_3\text{-}O)O_2)(\mu_2\text{-}O_2P(CH_2C_6H_5)_2)_6$" using 4,4'-bipyridine were not successful presumably because of steric interactions and only **3** was synthesized with this ligand. Increasing the bridge length by use of the longer N^1,N^2-dipyrid-4-yl oxalamide did result in linkage of the trimers in **5**. These compounds consisted of a quasi-isosceles triangle for the V ions within the central core and contained some differences in the bond distances and angles between themselves and related clusters. Thermal decomposition studies revealed that the cluster core is stable in that the ligand to dissociate first is the loosely bonded terminal monodentate ligand followed by phosphinate dissociation.

Supplementary material

CCDC 1050764 and 1050765 contain the supplementary crystallographic data for **3** and **5**, respectively. These data can be obtained free of charge via https://summary.ccdc.cam.ac.uk/structure-summary-form, or from the Cambridge Crystallographic Data Centre, 12 Union Road, Cambridge CB2 1EZ, UK; Fax: (+44) 1223-336-033; or E-mail: deposit@ccdc.cam.ac.uk. Figures S1-S7; FTIR and NMR data for **3** and **5**. Tables S1 and S2 for bond valence sum calculations on **3** and **5**, respectively.

Acknowledgements

MZ acknowledges the National Science Foundation for funding for X-ray diffraction equipment (grant CHE 0087210), the Ohio Board of Regents Grant CAP-491, and by Youngstown State University.

Disclosure statement

No potential conflict of interest was reported by the authors.

References

[1] F.A. Walker, R.L. Carlin, P.H. Rieger. *J. Chem. Phys.*, **45**, 4181 (1966).

[2] M. Sutradhar, G. Mukherjee, M.G.B. Drew, S. Ghosh. *Inorg. Chem.*, **45**, 5150 (2006).

[3] M. Jordan, W. Saak, D. Haase, R. Beckhaus. *Organometallics*, **29**, 5859 (2010).

[4] J.S. Maass, Z. Chen, M. Zeller, F. Tuna, R.E.P. Winpenny, R.L. Luck. *Inorg. Chem.*, **51**, 2766 (2012).

[5] J.S. Maass, Z. Chen, M. Zeller, R.L. Luck. *Dalton Trans.*, **40**, 11356 (2011).

[6] B.-C. Tzeng, Y.-F. Chen, C.-C. Wu, C.-C. Hu, Y.-T. Chang, C.-K. Chen. *New J. Chem.*, **31**, 202 (2007).

[7] W. Hsu, H.-L. Hsiao, J.-D. Chen. *Acta Crystallogr., Sect. E: Struct. Rep. Online*, **66**, o2873 (2010).

[8] J. Qin, J. Dong, J. Li, Y. Gong. *Acta Crystallogr., Sect. E: Struct. Rep. Online*, **66**, m743 (2010).

[9] V. Vajpayee, Y.H. Song, Y.J. Yang, S.C. Kang, H. Kim, I.S. Kim, M. Wang, P.J. Stang, K.-W. Chi. *Organometallics*, **30**, 3242 (2011).

[10] V. Vajpayee, Y.H. Song, M.H. Lee, H. Kim, M. Wang, P.J. Stang, K.-W. Chi. *Chem.-Eur. J.*, **17**, 7837 (2011).

[11] S.-L. Huang, Y.-J. Lin, Z.-H. Li, G.-X. Jin. *Angew. Chem., Int. Ed.*, **53**, 11218 (2014).

[12] S.-L. Huang, Y.-J. Lin, T.S.A. Hor, G.-X. Jin. *J. Am. Chem. Soc.*, **135**, 8125 (2013).

[13] M.-C. Dul, E. Pardo, R. Lescouëzec, Y. Journaux, J. Ferrando-Soria, R. Ruiz-García, J. Cano, M. Julve, F. Lloret, D. Cangussu, C.L.M. Pereira, H.O. Stumpf, J. Pasán, C. Ruiz-Pérez. *Coord. Chem. Rev.*, **254**, 2281 (2010).

[14] R. Ruiz, J. Faus, F. Lloret, M. Julve, Y. Journaux. *Coord. Chem. Rev.*, **193–195**, 1069 (1999).

[15] E.A. Boyd, M.E.K. Boyd, F. Kerrigan. *Tetrahedron Lett.*, **37**, 5425 (1996).

[16] R.A. Rowe, M.M. Jones. *Inorg. Synth.*, **5**, 113 (1957).

[17] M.M. Jones. *J. Am. Chem. Soc.*, **76**, 5995 (1954).

[18] Bruker, in: Apex2 v2.1-4, Bruker AXS Inc., Madison, WI, USA (2007).

[19] G.M. Sheldrick, T.R. Schneider, R.M.S. Charles W. Carter Jr, [16] SHELXL: High-resolution refinement, in: Methods in Enzymology, Academic Press, 1997, pp. 319.

[20] A.L. Spek. *Acta Crystallogr., Sect. C: Struct. Chem.*, **71**, 9 (2015).

[21] C.F. Macrae, I.J. Bruno, J.A. Chisholm, P.R. Edgington, P. McCabe, E. Pidcock, L. Rodriguez-Monge, R. Taylor, J. van de Streek, P.A. Wood. *J. Appl. Crystallogr.*, **41**, 466 (2008).

[22] A.S. Wills, VaList, Program available from www.ccp14.ac.uk/solution/bond_valence/.

Table 1. Crystal data and refinement details for **3** and **5**.

Compound reference	**3**	**5**
Chemical formula	$C_{94}H_{92}N_2O_{15}P_6V_3\cdot 2(CH_2Cl_2)$	$C_{180}H_{178}N_4O_{32}P_{12}V_6$
Formula mass	1998.19	3586.55
Crystal system	Monoclinic	Monoclinic
a/Å	13.664(1)	13.527(1)
b/Å	25.876(1)	25.792(2)
c/Å	27.405(1)	30.742(3)
β/°	102.212(1)	97.780(1)
Unit cell volume/Å^3	9470.3(9)	10627(2)
Temperature/K	100(2)	100(2)
Space group	$P2_1/n$	$P2_1/c$
No. of formula units per unit cell, Z	4	2
Absorption coefficient, μ/mm^{-1}	0.569	0.403
No. of reflections measured	131496	82712
No. of independent reflections	23492	26236
R_{int}	0.0289	0.0472
Final R_1 values ($I > 2\sigma(I)$)	0.0361	0.0533
Final $wR(F^2)$ values ($I > 2\sigma(I)$)	0.0909	0.1358
Final R_1 values (all data)^a	0.0451	0.0797
Final $wR(F^2)$ values (all data)^b	0.0987^c	0.1458^d
Goodness of fit on F^2	1.055	1.055
CCDC number	1050764	1050765

$^aR_1 = \sum||F_o| - |Fc||/\sum|F_o|$. $^bwR_2 = [\sum[w(F_o^2 - F_c^2)^2]/\sum[w(F_o^2)^2]]^{1/2}$. ^{c}w = $1/[\sigma^2(Fo^2) + (0.0439P)^2 + 8.2522P]$ where $P=(Fo^2+2(Fc)^2)/3$. ^{d}w = $1/[\sigma^2(Fo^2) + (0.0747P)^2]$.

Table 2. Selected bond distances and angles for **3**.

Bond distances (Å)					
V(1)-O(1)	1.6223(12)	V(2)-O(7)	2.0196(12)	O(7)-P(2)	1.5182(12)
V(1)-O(15)	1.9833(12)	V(3)-O(3)	1.5903(12)	O(8)-P(3)	1.5162(11)
V(1)-O(4)	1.9884(12)	V(3)-O(9)	1.9706(12)	O(9)-P(3)	1.5265(12)
V(1)-O(6)	2.0044(12)	V(3)-O(14)	1.9870(12)	O(10)-P(4)	1.5247(12)
V(1)-O(13)	2.0264(12)	V(3)-O(12)	1.9976(12)	O(11)-P(4)	1.5164(12)
V(1)-N(1)	2.4094(15)	V(3)-O(11)	2.0010(12)	O(12)-P(5)	1.5214(12)
V(2)-O(2)	1.5916(12)	O(4)-P(1)	1.5208(12)	O(13)-P(5)	1.5271(12)
V(2)-O(5)	1.9888(12)	O(5)-P(1)	1.5237(12)	O(14)-P(6)	1.5277(12)
V(2)-O(10)	1.9913(12)	O(6)-P(2)	1.5227(12)	O(15)-P(6)	1.5210(12)
V(2)-O(8)	2.0088(11)				
Bond angles (°)					
O(1)-V(1)-O(15)	99.66(5)	O(2)-V(2)-O(5)	101.35(6)	O(3)-V(3)-O(9)	105.41(6)
O(1)-V(1)-O(4)	100.12(5)	O(2)-V(2)-O(10)	104.83(6)	O(3)-V(3)-O(14)	105.67(6)
O(15)-V(1)-O(4)	160.11(5)	O(5)-V(2)-O(10)	153.82(5)	O(9)-V(3)-O(14)	148.89(5)
O(1)-V(1)-O(6)	96.84(5)	O(2)-V(2)-O(8)	97.54(6)	O(3)-V(3)-O(12)	98.77(6)
O(15)-V(1)-O(6)	87.93(5)	O(5)-V(2)-O(8)	87.39(5)	O(9)-V(3)-O(12)	87.10(5)
O(4)-V(1)-O(6)	87.69(5)	O(10)-V(2)-O(8)	89.28(5)	O(14)-V(3)-O(12)	86.90(5)
O(1)-V(1)-O(13)	96.83(5)	O(2)-V(2)-O(7)	97.42(6)	O(3)-V(3)-O(11)	97.44(6)
O(15)-V(1)-O(13)	91.00(5)	O(5)-V(2)-O(7)	90.24(5)	O(9)-V(3)-O(11)	88.53(5)
O(4)-V(1)-O(13)	88.70(5)	O(10)-V(2)-O(7)	86.34(5)	O(14)-V(3)-O(11)	88.81(5)
O(6)-V(1)-O(13)	166.27(5)	O(8)-V(2)-O(7)	165.02(5)	O(12)-V(3)-O(11)	163.79(5)
O(1)-V(1)-N(1)	177.46(6)				
O(15)-V(1)-N(1)	78.60(5)				
O(4)-V(1)-N(1)	81.70(5)	O(4)-P(1)-O(5)	115.22(7)	O(11)-P(4)-O(10)	115.62(7)
O(6)-V(1)-N(1)	84.97(5)	O(7)-P(2)-O(6)	115.95(7)	O(12)-P(5)-O(13)	114.04(7)
O(13)-V(1)-N(1)	81.40(5)	O(8)-P(3)-O(9)	115.84(7)	O(15)-P(6)-O(14)	115.50(7)

Table 3. Selected bond distances and angles for **5**.

Bond distances (Å)					
V(1)-O(1)	1.6243(16)	V(2)-O(7)	2.0152(17)	O(7)-P(2)	1.5145(17)
V(1)-O(4)	1.9904(17)	V(3)-O(3)	1.5869(19)	O(8)-P(3)	1.5092(18)
V(1)-O(15)	1.9995(17)	V(3)-O(9)	1.9762(19)	O(9)-P(3)	1.5197(17)
V(1)-O(6)	2.0019(17)	V(3)-O(14)	1.9885(19)	O(10)-P(4)	1.5207(17)
V(1)-O(13)	2.0217(18)	V(3)-O(11)	1.9956(18)	O(11)-P(4)	1.5015(19)
V(1)-N(1)	2.3846(19)	V(3)-O(12)	1.9980(18)	O(12)-P(5)	1.523(2)
V(2)-O(2)	1.5895(17)	O(4)-P(1)	1.5173(17)	O(13)-P(5)	1.5222(19)
V(2)-O(10)	1.9869(17)	O(5)-P(1)	1.5173(17)	O(14)-P(6)	1.5205(17)
V(2)-O(5)	1.9875(18)	O(6)-P(2)	1.5164(16)	O(15)-P(6)	1.5104(19)
V(2)-O(8)	1.9993(17)				
Bond angles (°)					
O(1)-V(1)-O(4)	99.22(8)	O(2)-V(2)-O(10)	103.28(8)	O(3)-V(3)-O(9)	106.29(9)
O(1)-V(1)-O(15)	99.21(8)	O(2)-V(2)-O(5)	101.51(8)	O(3)-V(3)-O(14)	105.27(9)
O(4)-V(1)-O(15)	161.44(7)	O(10)-V(2)-O(5)	155.20(7)	O(9)-V(3)-O(14)	148.44(8)
O(1)-V(1)-O(6)	97.11(8)	O(2)-V(2)-O(8)	97.67(8)	O(3)-V(3)-O(11)	98.28(9)
O(4)-V(1)-O(6)	87.13(7)	O(10)-V(2)-O(8)	89.66(7)	O(9)-V(3)-O(11)	88.06(8)
O(15)-V(1)-O(6)	88.43(7)	O(5)-V(2)-O(8)	86.93(7)	O(14)-V(3)-O(11)	87.62(8)
O(1)-V(1)-O(13)	96.74(8)	O(2)-V(2)-O(7)	97.73(8)	O(3)-V(3)-O(12)	99.78(9)
O(4)-V(1)-O(13)	88.56(7)	O(10)-V(2)-O(7)	86.34(7)	O(9)-V(3)-O(12)	87.80(8)
O(15)-V(1)-O(13)	91.46(7)	O(5)-V(2)-O(7)	90.49(7)	O(14)-V(3)-O(12)	86.74(8)
O(6)-V(1)-O(13)	165.99(7)	O(8)-V(2)-O(7)	164.59(7)	O(11)-V(3)-O(12)	161.92(7)
O(1)-V(1)-N(1)	178.93(8)				
O(4)-V(1)-N(1)	81.81(7)				
O(15)-V(1)-N(1)	79.78(7)	O(4)-P(1)-O(5)	114.31(10)	O(11)-P(4)-O(10)	116.03(10)
O(6)-V(1)-N(1)	83.20(7)	O(7)-P(2)-O(6)	116.04(10)	O(13)-P(5)-O(12)	114.70(10)
O(13)-V(1)-N(1)	82.99(7)	O(8)-P(3)-O(9)	115.83(10)	O(15)-P(6)-O(14)	115.32(10)

Table 4. Comparison of selected bond distances and angles for the core geometry in **3**, **5** (major component at 60.6% for $(V_3(\mu_3\text{-}O)O_2)(\mu_2\text{-}O_2P(CH_2C_6H_5)_2)_6H_2O)$, **1**, and one of the molecules for $(V_3(\mu_3\text{-}O)O_2)(\mu_2\text{-}O_2P(CH_2C_6H_5)_2)_6py$, **2**.

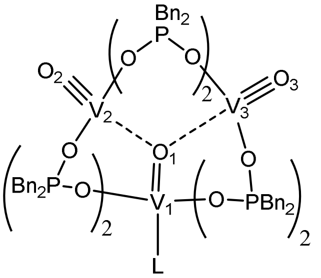

	1, L=H_2O	**2**, L=py	**3**, L=bipy	**5**, L=$(pyNCO)_2$
Distances (Å)				
V_1-O_1	1.60(2)	1.625(2)	1.622(1)	1.624(2)
V_2-O2	1.572(3)	1.588(2)	1.592(1)	1.590(2)
V_3-O_3	1.562(3)	1.584(2)	1.590(1)	1.587(2)
V_1-L	2.307(4)	2.350(3)	2.409(2)	2.385(2)
V_2-O_1	2.57(2)	2.510(2)	2.570(1)	2.526(2)
V3-O_1	2.74(2)	2.830(3)	2.728(1)	2.817(2)
$V_1\cdots V_2$	3.742(2)	3.738(1)	3.7766(4)	3.754(1)
$V_1\cdots V_3$	3.830(3)	3.917(1)	3.8286(4)	3.872(1)
$V_2\cdots V_3$	4.422(2)	4.409(1)	4.3849(4)	4.455(1)
Bond angles (°)				
O_1-V_1-L	179.8(6)	177.0(1)	177.46(6)	178.93(8)
V_1-O_1-V_2	125.8(9)	128.1(1)	127.06(6)	128.18(9)
V_1-O_1-V_3	121.6(8)	120.7(1)	121.20(5)	118.87(8)
V_2-O_1-V_3	112.6(6)	111.15(9)	111.68(4)	112.87(6)
V_2-V_1-V_3	71.45(4)	70.28(2)	70.41(1)	71.47(1)
V_1-V_3-V_2	53.35(3)	52.95(1)	54.24(1)	53.03(1)
V_1-V_2-V_3	55.20(3)	56.7(1)	55.35(1)	55.50(1)

[a] Distances and angles for **3** and **5** not in tables 2 and 3 were obtained using Mercury [21]. Those for **1** and **2** were taken from table 4 in reference [4].

Figure captions

Figure 1. Mercury [21] thermal ellipsoid (50%) representation of **3** showing the main molecule. Solvent molecules of crystallization are not depicted and hydrogens are represented by spheres of arbitrary radii.

Figure 2. Mercury [21] thermal ellipsoid (50%) representation of **5** showing the main molecule. Solvent molecules of crystallization are not depicted and hydrogens have been omitted for clarity.

Figure 3. TGA curve of $(V_3(\mu_3\text{-}O)O_2)(\mu_2\text{-}O_2P(CH_2C_6H_5)_2)_6(4,4'\text{-bpy})$, **3**, at a heating rate of 10 °C/min.

Figure 4. TGA curve of $((V_3(\mu_3\text{-}O)O_2)(\mu_2\text{-}O_2P(CH_2C_6H_5)_2)_6)_2$(*N*,*N*'-4-dipyridyl oxalamide), **5**, at a heating rate of 10 °C/min.

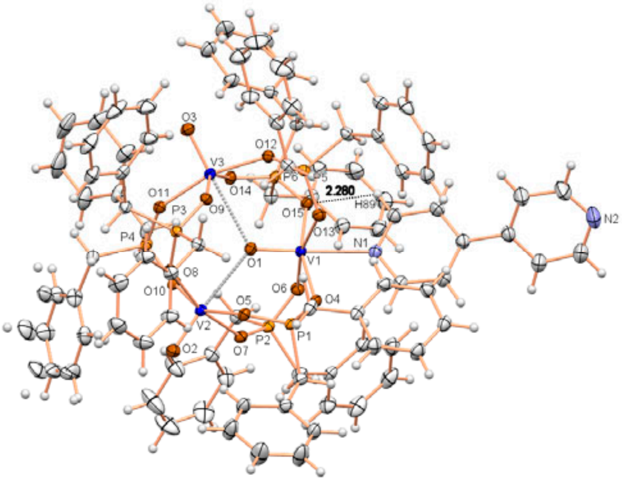
O3
V3
O12
P6
O14
2.280
O11
P3
O9
O15
H89
O13
N2
P4
O1
V1
N1
O8
O10
O6
O4
O5
V2
P2
P1
O2
O7

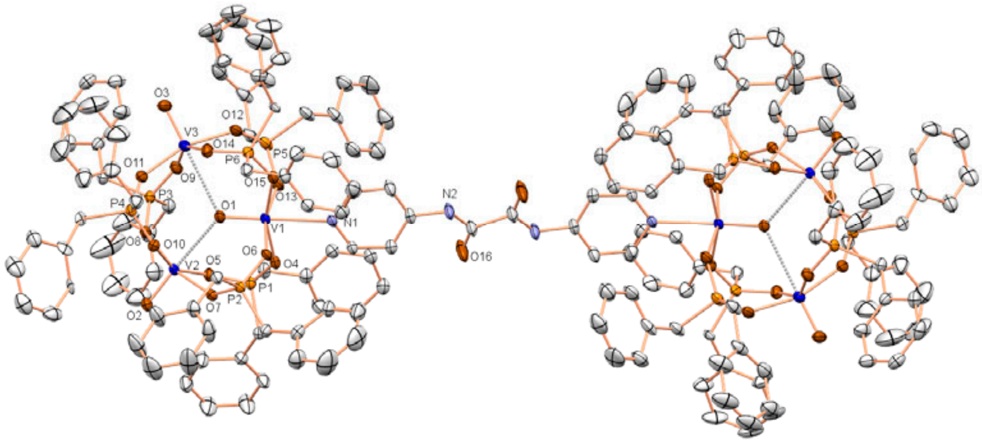
O3
V3
O12
O14
P6
P5
O11
O9
O15
O13
P4
P3
O1
V1
N1
N2
O8
O10
V2
O5
O6
O4
O16
O2
O7
P2
P1

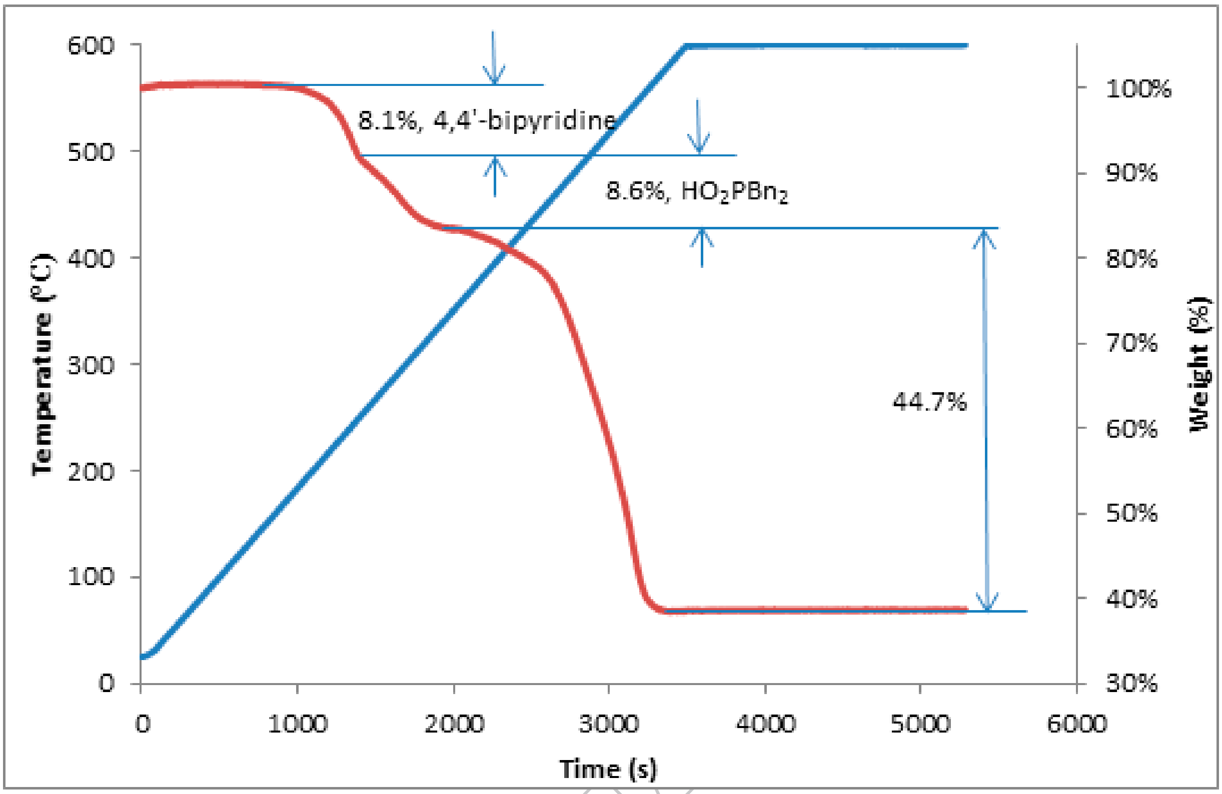
8.1%, 4,4'-bipyridine
8.6%, HO_2PBn_2
44.7%
Temperature (°C)
Weight (%)
Time (s)
0
100
200
300
400
500
600
0
1000
2000
3000
4000
5000
6000
30%
40%
50%
60%
70%
80%
90%
100%

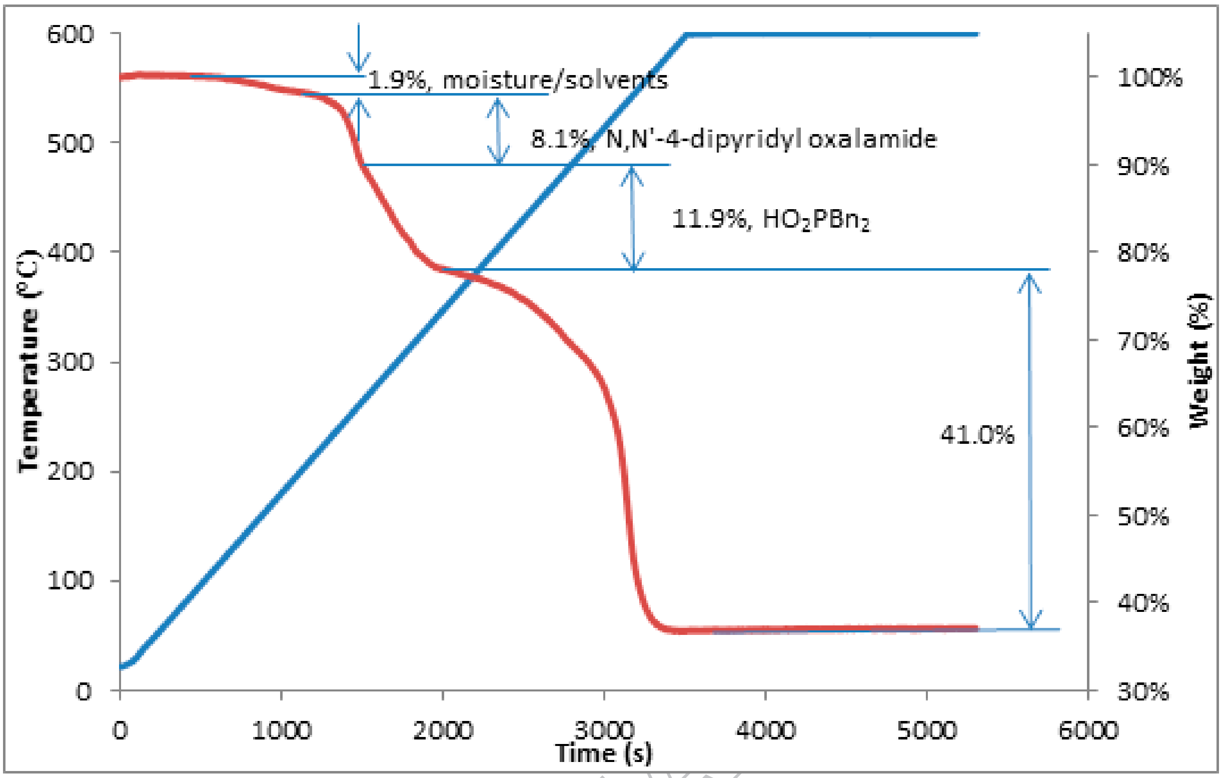
600
500
400
300
200
100
0
Temperature (°C)
0
1000
2000
3000
4000
5000
6000
Time (s)
100%
90%
80%
70%
60%
50%
40%
30%
Weight (%)
1.9%, moisture/solvents
8.1%, N,N'-4-dipyridyl oxalamide
11.9%, HO₂PBn₂
41.0%